

Article

Adaptation of Signal with NOMA and Polar Codes to the Rayleigh Channel

Dmitriy Pokamestov ^{1,*}, Yakov Kryukov ¹, Eugeni Rogozhnikov ¹, Georgiy Shalin ¹, Artem Shinkevich ¹ and Serafim Novichkov ²

¹ Department of Telecommunications and Basic Principles of Radio Engineering, Tomsk State University of Control and Radioelectronics, 634045 Tomsk, Russia

² Skolkovo Institute of Science and Technology, 446411 Moscow, Russia

* Correspondence: dmitrii.a.pokamestov@tusur.ru

Abstract: Polar codes are one of the most effective methods of error correction coding. Currently, these codes are used in 5G communication systems and are the main candidate for 6G. Symmetry plays an important role in coding and decoding algorithms for polar codes. Modulation and multiple access methods are the basis for a physical layer along with error correction codes. Non-Orthogonal Multiple Access (NOMA) methods are a promising technology for future telecommunication systems. They allow the increase of both spectral efficiency and the quantity of subscribers of a communication system. In this paper, we consider a communication system with polar codes, traditional orthogonal multiple access (OMA), and NOMA. The channel with multipath propagation, which can be defined by the Rayleigh channel model, is especially difficult to transmit. We propose a method for adapting signals with polar codes to a channel state based on the analysis of channel matrix and permutation of logical subchannels. The results obtained demonstrate efficiency compared to classical solutions and do not really increase the computational complexity of signal processing and decoding.

Keywords: polar codes; NOMA; PD-NOMA; 5G; 6G; Rayleigh fading channel; adaptation



Citation: Pokamestov, D.; Kryukov, Y.; Rogozhnikov, E.; Shalin, G.; Shinkevich, A.; Novichkov, S.

Adaptation of Signal with NOMA and Polar Codes to the Rayleigh

Channel. *Symmetry* **2022**, *14*, 2103.

<https://doi.org/10.3390/sym14102103>

Academic Editors: Pingping Chen, Yi Fang, Long Shi and Jan Awrejcewicz

Received: 31 August 2022

Accepted: 7 October 2022

Published: 10 October 2022

Publisher's Note: MDPI stays neutral with regard to jurisdictional claims in published maps and institutional affiliations.



Copyright: © 2022 by the authors. Licensee MDPI, Basel, Switzerland. This article is an open access article distributed under the terms and conditions of the Creative Commons Attribution (CC BY) license (<https://creativecommons.org/licenses/by/4.0/>).

1. Introduction

Polar codes are a relatively new type of error correction coding proposed by Arıcan in [1]. It has been shown that polar codes are the first family of codes capable of reaching the bandwidth of binary-input discrete memoryless channels (BDMC) with a low computational complexity of decoding, which can be estimated as $O(n \log n)$, where n is the codeword length, at the same time. Despite its novelty, the concept of polar codes has found practical use in the fifth-generation communication systems (5G NR) [2], where they are used in the BCH (Broadcast Channel) transport channel and with DCI and UCI (Downlink and Uplink Control Information). In addition, a number of articles consider them as the main candidate for the role of forward error correction scheme for 6G networks [3–5]. Polar codes are promising for use in channels with low latency [3]; they allow for flexible control of the encoding rate and the length of code words [4].

The idea of applying polar codes is to split bit-channels into the most and least reliable ones. The most reliable channels are used to transmit information bits and the least reliable ones are considered frozen, which means that zero values are recorded in them when forming code words. The reliability sequence of bits depends on the way the polar codes are constructed. Despite the fact that most papers consider the classical block structure proposed in [1], there are methods for constructing convolutional polar codes [6]. In addition, polar codes are used together with others to form a concatenated code [7] to increase efficiency. Thus, in 5G NR, a cyclic redundancy check (CRC) is calculated before polar encoding, which significantly increases the transmission noise immunity [8].

Modern communication systems operate under complex conditions of multipath propagation. Mathematically, this phenomenon can be represented as the Rayleigh fading

channel model. The communication standards contain recommended parameters for such models, for example, the TDLA-30 scenario in 5G NR [9]. Such channels are characterized by deep fading resulting in an increase in the likelihood of error in the data transmitted in these areas. Thus, different subcarriers in orthogonal frequency division multiple access may have a different signal noise ratio (SNR): up to 20 dB or greater.

Papers [10–12] discuss the construction of polar codes, taking into account the features of channel models. Reference [12] is of the greatest interest as it shows how the Rayleigh channel is reduced to the case of a binary input additive white Gaussian noise channel (BI-AWGN) using Gaussian approximation and Kullback–Leibler divergence, and polar codes are constructed for it in accordance with [7]. However, the algorithms in this paper are quite complicated and cannot be performed in real time, taking into account the non-stationarity of the channel. The algorithms proposed in these works are very computationally complex and are not adapted for use in modern FPGAs, DSPs or ASICs. That is why the 5G standard describes a fairly simple channel coding sequence that almost ignores the current state of the transmission channel [8]. We propose a simple modification of channel coding using polar codes based on the additional sorting of the reliability of physical channels, for example, orthogonal frequency-division multiplexing (OFDM) subcarriers. Bit channels of polar codes have a different reliability, while in practice, all transmitted information bits should have a minimum bit error probability. Our idea is to align the reliability of the transmission of all information bits by considering the state of both physical and bit channels simultaneously. It can be achieved by including an additional interleaver that distributes encoded bits over optimal physical channels in the channel coding scheme. We present the results of noise immunity, demonstrating the benefits of this approach. Additionally, we investigate the effect of the channel estimation error on the proposed method. Due to its simplicity, the computational complexity of signal formation and processing algorithms increases insignificantly, so the method under consideration can be easily applied in practice in existing communication systems.

As part of the discussion on the 5G standard, a new approach to the formation of physical subchannels has been proposed, that is, the non-orthogonal multiple access (NOMA). Contrary to the orthogonal multiple access (OMA), NOMA implies simultaneous transmission of signals by subscribers in the same time–frequency resource. Several implementations of NOMA principles have been proposed: power division (PD-NOMA) [13], sparse code multiple access (SCMA) [14], rate splitting multiple access (RSMA) [15], etc. [16], which differ from each other in the principles of signal formation and separation (demodulation). It is shown that NOMA surpasses traditional methods based on OFDM in noise immunity and spectral efficiency. Therefore, NOMA is the main candidate for the physical layer architecture in 6G. It should be noted that 6G discussions are at an early stage; a specific NOMA technique has not been selected and the above-described technologies (PD-NOMA, RSMA, SCMA, etc.) continue to compete with each other [17]. NOMA combines multiple access and modulation procedures. Together with error correction coding, NOMA forms the basis of the physical layer and largely determines the main characteristics of the future communication networks. Thus, in this article we consider polar codes together with NOMA (PD-NOMA is chosen as an example) and, therefore, propose a physical layer concept for the next-generation communication networks. PD-NOMA topics are actively developing, with real applications within non-orthogonal multiple access technique operating communication systems, such as user association and contract-theoretic resource orchestration [18]. A relevant application of PD-NOMA is in simultaneous wireless information and power transfer (SWIPT) [19].

The article is structured as follows. Section 2 contains the description of the model under consideration and provides basic theory on the polar code and NOMA technologies used. In Section 3, we describe the proposed method of adapting polar codes to the transmission channel state for systems with OMA and NOMA. The fourth section is devoted to the simulation scenario and its results using the Monte Carlo method. We consider the transmission in the Rayleigh fading channel. The following designations are

accepted in the work: \mathbb{B} , \mathbb{R} , \mathbb{C} denote binary, real, and complex numbers. To denote scalars, vectors and matrices, x , \mathbf{x} , and \mathbf{X} notations are used, respectively; the j -th column of \mathbf{X} is denoted $\mathbf{X}^{(j)}$; the i -th row of \mathbf{X} is denoted $\mathbf{X}_{(i)}$; x_{ij} is X element at the intersection of the i -th row and the j -th column; $\|\mathbf{x}\|$ is the norm of vector \mathbf{x} ; and \mathbf{I}_L is a unit matrix of $L \times L$ size.

2. System Model

In this paper, we consider two types of communication channels: with OMA (Figure 1) including one transmitter and one receiver, and with NOMA (Figure 2) including one transmitter and two receivers—user equipment (UE) 1 and 2.

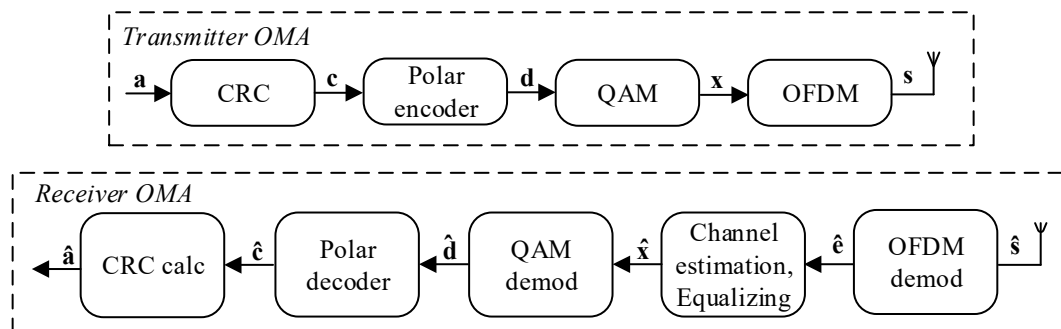


Figure 1. OMA channel with polar code.

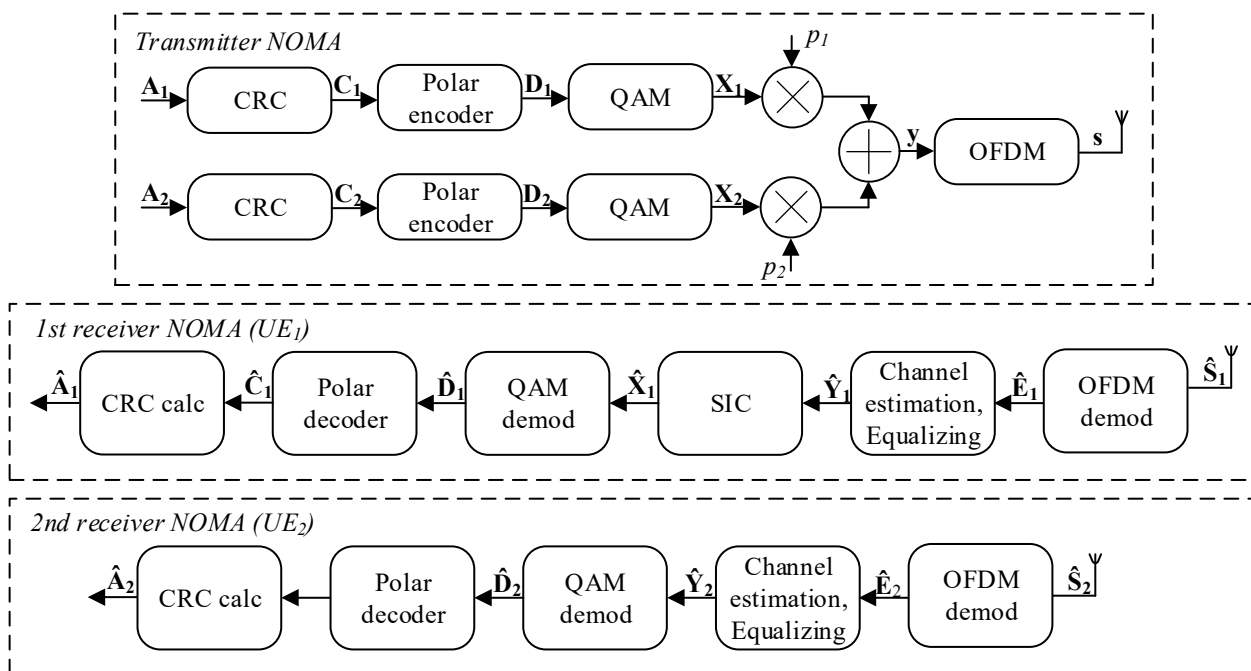


Figure 2. NOMA channel with polar code.

Table 1 shows the designations of the main vectors used in the model. Both types of channels (Figures 1 and 2) use CRC (polynomials according to [2] of length L from 6 to 26.), input bits \mathbf{a} , and output bits \mathbf{c} (C_1 , C_2). Both channels use quadrature amplitude modulation (QAM) with index M , and symbols at the output \mathbf{x} , \mathbf{X}_1 , \mathbf{X}_2 . In the NOMA channel, the group signal is designated as \mathbf{y} . The last stage is OFDM with output values \mathbf{s} . The estimates of the corresponding values in the receiver after the processing stages are denoted as $\hat{\mathbf{a}}$, $\hat{\mathbf{A}}_1$, $\hat{\mathbf{c}}$, $\hat{\mathbf{C}}_1$, etc.

Table 1. Characteristics of the simulation model for OMA and (NOMA) channel.

Vectors Name	Dimensionality of Vectors	Explanation
a ($\mathbf{A}_1, \mathbf{A}_2$)	$K-L$	Bitstream at the input of the OMA transmitter (1st and 2nd NOMA subscribers)
c ($\mathbf{C}_1, \mathbf{C}_2$)	K	Bitstream with CRC
d ($\mathbf{D}_1, \mathbf{D}_2$)	N	Bitstreams after polar coding
x ($\mathbf{X}_1, \mathbf{X}_2$)	$N/\log_2(M)$	Modulation symbols
y	$N/\log_2(M)$	NOMA group symbols
\hat{s} ($\hat{\mathbf{S}}_1, \hat{\mathbf{S}}_2$)	$N/\log_2(M)$ + cyclic prefix	OFDM symbol
\hat{e} ($\hat{\mathbf{E}}_1, \hat{\mathbf{E}}_2$)	$N/\log_2(M)$	Received symbols in the frequency domain
H	$N/\log_2(M) \times 1$	Channel matrix
N	$N/\log_2(M)$	AWGN sample vector
t ($\mathbf{T}_1, \mathbf{T}_2$)	N	Interleaved Bits
R	$N \times N$	Interleaver matrix

In the model, we consider a multipath transmission channel with channel matrix $\mathbf{H} = (h_i), h_i \sim CN(0,1), i = 1, \dots, N/\log_2(M)$ and additive white Gaussian noise $\mathbf{N} = (n_{ij}), n_{ij} \sim CN(0, N_0)$, where N_0 is noise variance. The signal in the frequency domain at the input of the OMA receiver can be described as:

$$\hat{\mathbf{e}} = \text{diag}(\mathbf{H})\mathbf{x} + \mathbf{N}. \tag{1}$$

For NOMA:

$$\hat{\mathbf{E}}_i = \text{diag}(\mathbf{H}_i)\mathbf{X}_i + \mathbf{N}_i, i = 1, 2, \tag{2}$$

where $\mathbf{H} = (h_j), j = 1, \dots, \frac{N}{\log_2 M}; \mathbf{H} \sim CN(0,1)$ is the channel matrix; $\mathbf{N} = (n_j), j = 1, \dots, \frac{N}{\log_2 M}; \mathbf{N} \sim CN(0, N_0)$ are vectors with spectral counts of noise releases; N_0 is spectral noise power density; $\mathbf{H}_i, \mathbf{N}_i$ are similar parameters for two NOMA subscribers.

2.1. Polar Codes

Polar encoder (N, K) converts message vector $\mathbf{c} = (c_j)$ into code word \mathbf{d} as follows:

$$\mathbf{d} = \mathbf{u}\mathbf{G}_N \tag{3}$$

$$\mathbf{u} = (u_i), i = 1, \dots, N, u_i = c_j, \text{ if } i \notin \mathbf{F}, u_i = 0, \text{ if } i \in \mathbf{F} \mathbf{F} = (f_1, \dots, f_{N-K}) \tag{4}$$

$\mathbf{G}_N = (g_{ij}), i = 1, \dots, N, j = 1, \dots, N$, we use kernel $\mathbf{G}_2 = \begin{bmatrix} 1 & 0 \\ 1 & 1 \end{bmatrix}$, according to [1], and Kronecker product:

$$\mathbf{G}_N = \mathbf{G}_2^{\otimes n} = \begin{bmatrix} \mathbf{G}_{N/2} & 0 \\ \mathbf{G}_{N/2} & \mathbf{G}_{N/2} \end{bmatrix}. \tag{5}$$

For example, for $N = 4$, the generator matrix and encoding procedure are shown in Figure 3.

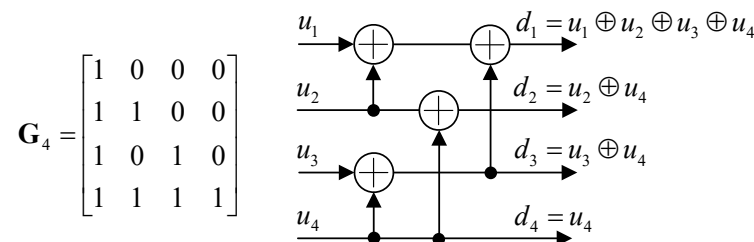


Figure 3. \mathbf{G}_4 and encoder for $N = 4$.

As can be seen from the structure of the generator matrix and encoder, the idea of symmetry is central. The concept of polar codes is based on polar transformation and

lies in splitting bit subchannels into channels with a minimum noise value (maximum noise-immune) and channels with a maximum noise value (minimum noise-immune). If $n \rightarrow \infty$, then it is possible to obtain a channel with absolute noise immunity (with bit error probability $P_e = 0$) and a totally noisy channel (with $P_e = 1$). The noise immunity of the u_i channel is determined by the number of test channels (bits) d_n , which it helps to form. Based on this fact, it is possible to make the reliability sequence $\mathbf{Q} = (q_i)$ of all N subchannels by calculating $\mathbf{V} = (V_{q_i})$, that is, the weights of the rows of matrix \mathbf{G}_N , and sorting them in ascending order:

$$\mathbf{Q} = (q_1, \dots, q_N); V_{q_i} = \sum_{j=1}^N g_{q_{ij}}; V_{q_1} < \dots < V_{q_i} < \dots < V_{q_N}; i = 1, \dots, N; q_i \in (1, \dots, N). \quad (6)$$

To form the encoder at $R=K/N$ rate, \mathbf{c} bits arriving at the encoder input are written to \mathbf{u} according to (2); moreover:

$$\mathbf{F} = (f_i) = (q_1, \dots, q_{N-K}). \quad (7)$$

Different versions of the successive-cancellation algorithm are used to decode polar codes [20]. This algorithm is based on the principles of fractals and symmetry. List decoding shows the greatest efficiency [21]. This algorithm also employs CRC [7]. During the decoding process, a list of L possible paths is saved in each iteration. At the end of decoding, hard decisions are compared with the corresponding CRC values and the most plausible one is selected.

2.2. NOMA

The next stage of signal generation is modulation. In the NOMA scenario (Figure 2), modulation and multiple access are combined into one process. In both OMA and NOMA, QAM-M is used. The main idea of NOMA is to simultaneously transmit X QAM characters to two or more subscribers [13]. Let us consider NOMA with two subscribers: a larger number will significantly increase the computational complexity of signal processing and it will not provide a significant gain. In this case, the group signal can be written as:

$$\mathbf{Y} = \sqrt{p_1}\mathbf{X}_1 + \sqrt{p_2}\mathbf{X}_2, \quad (8)$$

where p_1, p_2 are weighting factors responsible for the distribution of power between subscribers. The further away the subscriber is from the transmitter, the smaller its SNR is and the more power it will be allocated. To determine p_1 and p_2 , depending on the channel state, is one of the current problems in NOMA. One of the possible solutions is presented in [22]. We consider a scenario where UE1 is closer to the transmitter than UE2. Thus, $\text{SNR}_1 > \text{SNR}_2$, and $p_1 < p_2$. Figure 4 shows an example of signal constellations of two subscribers at $p_1 = 0.1, p_2 = 0.9$, and with QAM-16 modulation.

A number of publications [13,16,23] show that, due to the flexible distribution of power between subscribers, NOMA wins over OMA, which makes it an attractive technology for 6G systems.

Decoding NOMA characters in UE1 is performed using the successive interference cancellation algorithm (SIC) in two stages. During the first stage, a subscriber's signal \mathbf{X}_2 with a higher power is demodulated from $\hat{\mathbf{Y}}_1$. As a result, vector \mathbf{D}_2 is obtained. After that, \mathbf{X}_2 is restored from \mathbf{D}_2 and is subtracted from $\hat{\mathbf{Y}}_1$ with the corresponding weight:

$$\hat{\mathbf{X}}_1 = \frac{\hat{\mathbf{Y}}_1 - \sqrt{p_2}\mathbf{X}_2}{\sqrt{p_1}}. \quad (9)$$

UE2 demodulates the $\hat{\mathbf{Y}}_2$ signal based on the standard principles of QAM demodulation, while signal \mathbf{X}_1 contained in $\hat{\mathbf{Y}}_2$ is a system-inherent interference.

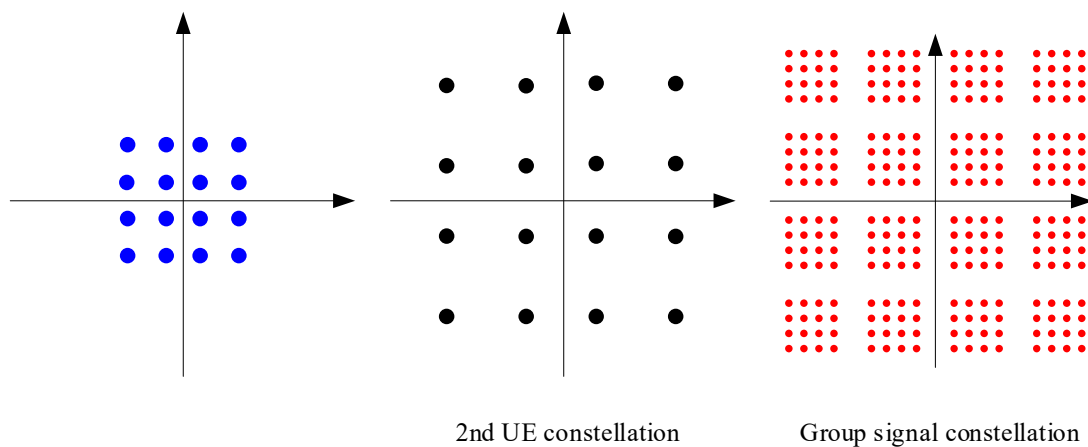


Figure 4. Forming group NOMA signal.

3. Adaptation of Signals with Polar Codes to Channel State

In accordance with (1) and (2), a signal passes through the multipath Rayleigh channel. To eliminate its influence, an equalization procedure is used in communication systems with OFDM. Zero forcing (ZF) and minimum mean squared error (MMSE) are the most widely used [24] for it. The signal after the ZF equalizer for the OMA scenario (Figure 1) can be described by the expression:

$$\hat{x}_i = \hat{e}_i \frac{\text{conj}(\hat{h}_i)}{|\hat{h}_i|^2}, \quad (10)$$

where $\hat{\mathbf{H}} = (\hat{h}_i)$ is an estimate of channel matrix \mathbf{H} . In vector form,

$$\hat{\mathbf{x}} = \hat{\mathbf{e}} \text{conj}(\text{diag}(\hat{\mathbf{H}})) (\text{conj}(\text{diag}(\hat{\mathbf{H}})) \text{diag}(\hat{\mathbf{H}}))^{-1}. \quad (11)$$

The signal after MMSE is described by the following expression:

$$\hat{x}_i = \hat{e}_i \frac{\text{conj}(\hat{h}_i)}{(|\hat{h}_i|^2 + N_0)}. \quad (12)$$

In vector form,

$$\hat{\mathbf{x}} = \hat{\mathbf{e}} \text{conj}(\text{diag}(\hat{\mathbf{H}})) (\text{conj}(\text{diag}(\hat{\mathbf{H}})) \text{diag}(\hat{\mathbf{H}}) + N_0 \mathbf{I})^{-1}. \quad (13)$$

The problem of both ZF and MMSE equalizers is noise amplification (SNR reduction) on subcarriers attributed to the deep fading region (low values of h_i). Thus, different frequency subchannels provide different SNR levels and, as a consequence, the bit error probability in them is different. This problem is especially acute for ZF, since it does not take into account information about the noise level in the channel.

The idea of adapting the transmission of signals with polar codes to the channel state is based on the combination of inhomogeneities of frequency subchannels and bit subchannels of polar codes. It is proposed to transmit logical subchannels containing information about the minimum number of information bits via physical channels with a low SNR ratio. Thus, the adaptation algorithm includes several steps:

Step 1. Sorting channel matrix elements in ascending order of the module:

$$\tilde{\mathbf{H}} = (\tilde{h}_i), \tilde{h}_i \in \hat{\mathbf{H}}, i = 1, \dots, N; |\tilde{h}_1| \leq |\tilde{h}_2| \leq \dots \leq |\tilde{h}_i| \leq \dots \leq |\tilde{h}_N|. \quad (14)$$

Forming index vector of sorted subcarriers:

$$\mathbf{W} = (w_i) \Big| \tilde{h}_{w_i} \equiv h_i, i = 1, \dots, N. \tag{15}$$

If the modulation with $M > 2$ is used, several logical streams are transmitted in each physical subchannel. In this case, each element of vector \mathbf{W} is repeated $\log_2(M)$ times.

Step 2. Counting the number of information bits contained in each logical subchannel (frozen bits are not taken into account in this stage):

$$v_j = \sum_{i \in (1 \dots N) \setminus \mathbf{F}} g_{ij}, \tag{16}$$

where g_{ij} are the elements of the generator matrix of polar code \mathbf{G} .

Forming the vector of indices of matrix \mathbf{V} sorted elements:

$$\mathbf{U} = (u_i) \Big| v_{u_1} \geq v_{u_2} \dots \geq v_{u_i} \dots \geq \dots v_{u_N}, i = 1, \dots, N. \tag{17}$$

Step 3. Interleaving bit subchannels so that channels containing the maximum number of information bits are transmitted over the most reliable physical subchannels and vice versa. This is provided by interleaving, permutation matrix $\mathbf{R} = (r_{ij})$, which, according to (15) and (17), contains values “1” at the intersection of the row with index w_i and the column with index u_i ; the remaining elements are equal to 0.

The interleaved vector of encoded bits can be written as:

$$\mathbf{t} = \mathbf{dR}. \tag{18}$$

Let us consider an example of the proposed method for $N = 8, K = 4$, and BPSK modulation. Let an OMA channel of eight subcarriers be given; modules of elements $|h_k|$ are shown in Figure 5a, and sorted elements $|\tilde{h}_k|$ are shown in Figure 5b.

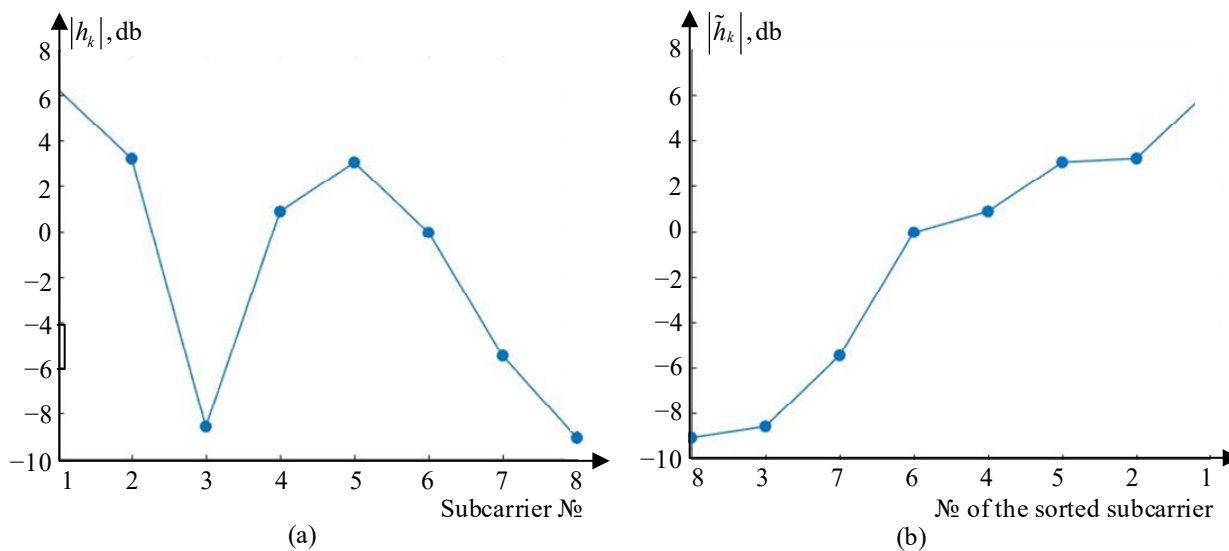


Figure 5. Channel matrix \mathbf{H} ; (a)—elements $|h_k|$; (b)—elements $|\tilde{h}_k|$.

In this case, the index vector of the sorted subcarriers is equal to $\mathbf{W} = [8 \ 3 \ 7 \ 6 \ 4 \ 5 \ 2 \ 1]$. At $N = 8$, matrix \mathbf{G} takes the following form:

$$\mathbf{G}_8 = \begin{bmatrix} 1 & 0 & 0 & 0 & 0 & 0 & 0 & 0 \\ 1 & 1 & 0 & 0 & 0 & 0 & 0 & 0 \\ 1 & 0 & 1 & 0 & 0 & 0 & 0 & 0 \\ 1 & 1 & 1 & 1 & 0 & 0 & 0 & 0 \\ 1 & 0 & 0 & 0 & 1 & 0 & 0 & 0 \\ 1 & 1 & 0 & 0 & 1 & 1 & 0 & 0 \\ 1 & 0 & 1 & 0 & 1 & 0 & 1 & 0 \\ 1 & 1 & 1 & 1 & 1 & 1 & 1 & 1 \end{bmatrix}.$$

The weight of the matrix columns is:

$$\mathbf{V} = [8 \ 4 \ 4 \ 2 \ 4 \ 2 \ 2 \ 1], N = 8, K = 8.$$

Taking into account frozen subchannels,

$$\mathbf{V} = [5 \ 3 \ 3 \ 2 \ 4 \ 2 \ 2 \ 1], N = 8, K = 4.$$

Then the vectors of the indices of sorted elements \mathbf{V} :

$$\mathbf{U} = [1 \ 5 \ 3 \ 2 \ 7 \ 6 \ 4 \ 8].$$

In this case, the permutation matrix takes the following form:

$$\mathbf{R} = \begin{bmatrix} 0 & 0 & 0 & 0 & 0 & 0 & 0 & 1 \\ 0 & 0 & 0 & 0 & 0 & 1 & 0 & 0 \\ 0 & 0 & 0 & 0 & 0 & 0 & 1 & 0 \\ 0 & 1 & 0 & 0 & 0 & 0 & 0 & 0 \\ 0 & 0 & 1 & 0 & 0 & 0 & 0 & 0 \\ 0 & 0 & 0 & 0 & 1 & 0 & 0 & 0 \\ 0 & 0 & 0 & 1 & 0 & 0 & 0 & 0 \\ 1 & 0 & 0 & 0 & 0 & 0 & 0 & 0 \end{bmatrix}.$$

The indicated above description of the method proposed above is valid for OMA systems. NOMA systems rely on the same general principles, but the adaptation is performed for each subscriber individually. As a result of applying the method, the diagrams shown in Figures 1 and 2 are transformed as demonstrated in Figure 6 (OMA) and Figure 7 (NOMA).

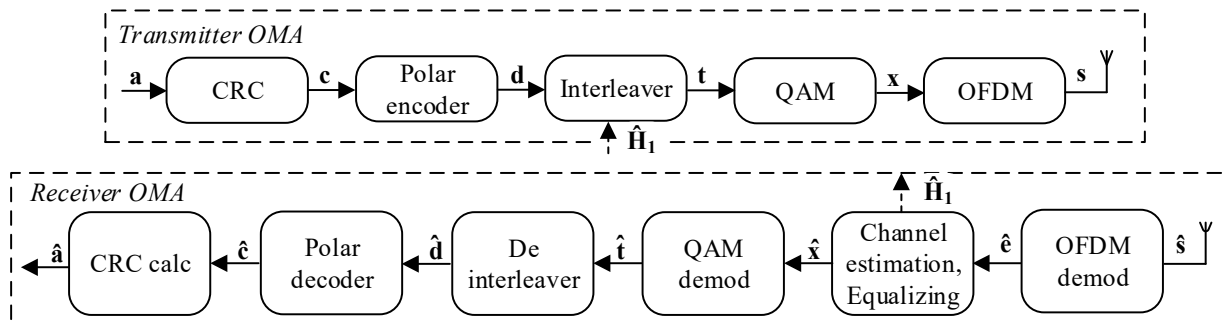


Figure 6. OMA channel with adapted polar code.

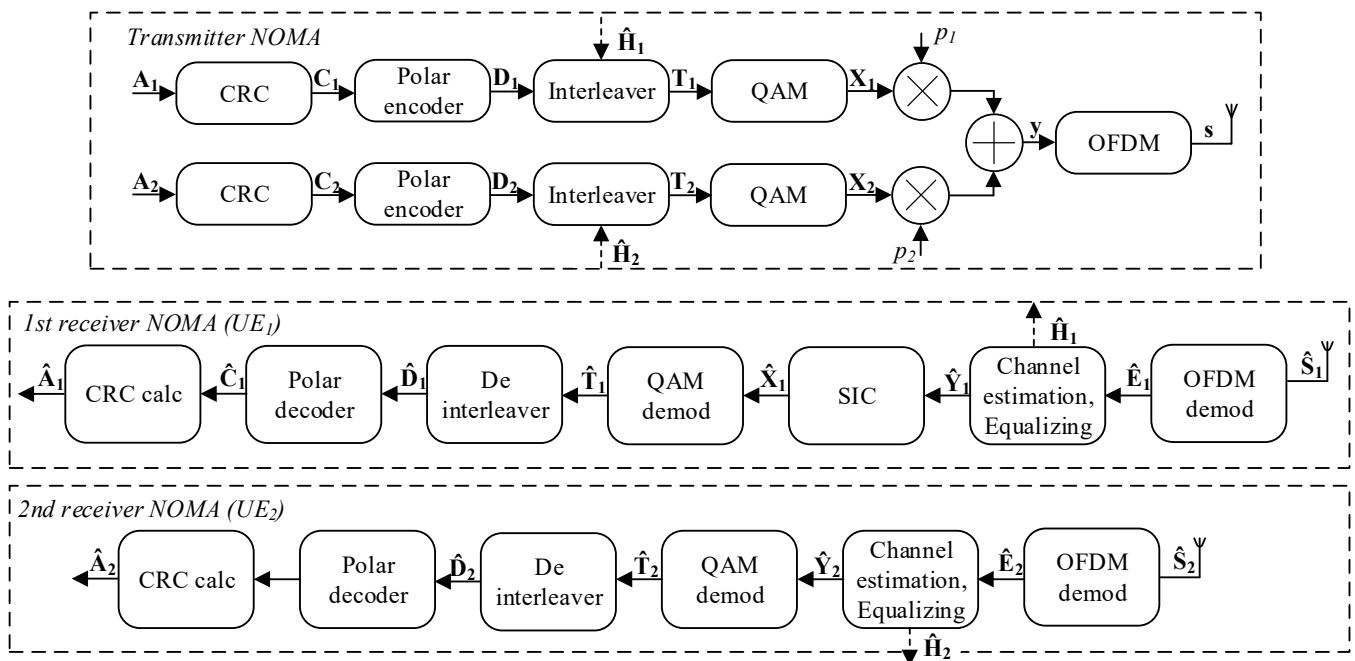


Figure 7. NOMA channel with adapted polar code.

We shall note that the estimation of channel matrix $\hat{\mathbf{H}}$ should arrive at the transmitter via the return service communication channel.

Separately, we shall note the computational complexity of signal processing in the classical method and the method proposed in this work. It is known that the computational complexity of polar decoding algorithms is estimated to be $O(n \log n)$.

The proposed method consists of sorting elements of the channel matrix, sorting bit subchannels in the order of their “importance” and the permutation of bit channels. Note that bit channel sorting is performed once and its complexity can be neglected. To adapt to the channel state, it is necessary to perform channel matrix sorting and channel permutation. The complexity of permutation can be described as $O(n)$. The complexity of sorting can be expressed as $O(n \log n)$. Thus, the total complexity of the algorithm is also $O(n \log n)$.

As the interval of temporal stationarity of the channel in the general case considerably exceeds duration of one OFDM symbol, the offered method has essentially smaller complexity in comparison with decoding. Thus, application of the method in practice will lead to insignificant growth of complexity.

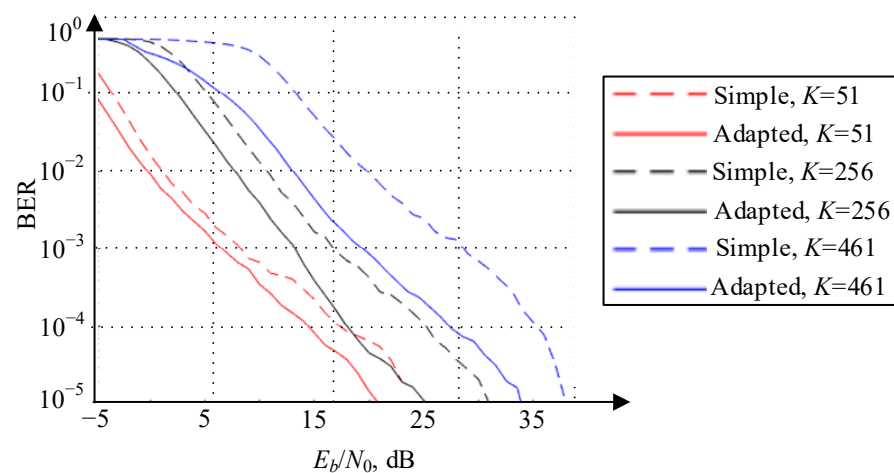
4. Simulation Results

The efficiency of the proposed methods is estimated with the help of a simulation using the Monte Carlo method. Summary parameters of the model are given in Table 2. First, we consider the OMA system implemented according to the schemes in Figures 1 and 6. It should be noted that, in the simulation, we do not apply the most effective ZF equalizer, which, however, allows us to demonstrate the results of the method more clearly. Using other equalization methods requires that adjustments are made to sorting (14)–(17).

Figure 8 shows the dependencies of the bit error rate (BER) performance on energy per bit to noise power spectral density ratio (E_b/N_0) for different encoding rates ($R \approx 1/10, 1/2, 9/10$) with BPSK modulation when transmitting in the Rayleigh channel with random values of elements \mathbf{H} , ZF equalizer, using the proposed method (Adapted) or without it (Simple). In this scenario, the receiver ideally estimates the channel, and $\hat{\mathbf{H}} = \mathbf{H}$.

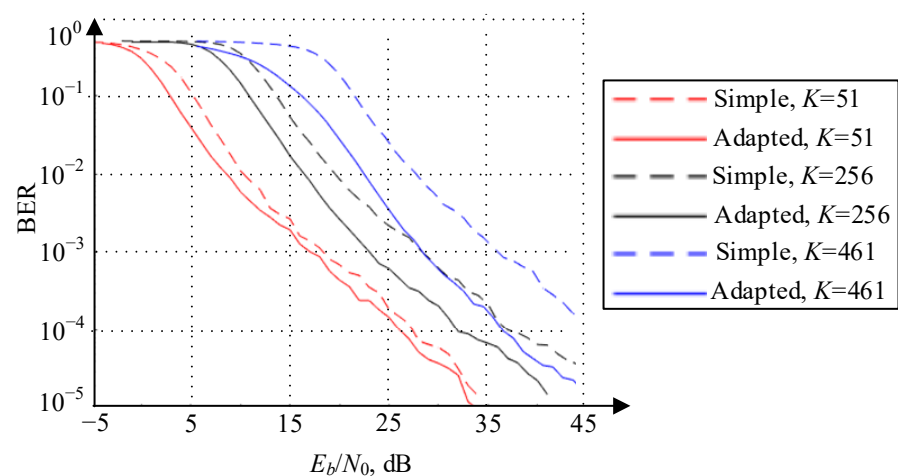
Table 2. Characteristics of the simulation model.

Characteristics of the Simulation Model	Value
Access type	NOMA, OMA
N	512
K	51, 259, 451
Modulation type	BPSK, QPSK, 16QAM
CRC polynomial	$g_{\text{CRC11}}(D) = [D^{11} + D^{10} + D^9 + D^5 + 1]$
Multipath channel type	Rayleigh (random)
Equalizer type	ZF

**Figure 8.** BER performance for different polar codec rates, BPSK modulation.

As can be seen from Figure 8, the use of the adaptation method significantly reduces the bit error probability. Depending on the encoding rate and BER value, the gain ranges from ≈ 3 dB to more than 5 dB.

Figure 9 shows the BER performance dependencies for QAM-16 modulation. The other transmission characteristics correspond to the previous scenario. An increase in the modulation index provides a greater rate, but also leads to an increase in the error probability.

**Figure 9.** BER performance of the OMA system for different polar codec rates, 16QAM modulation.

As in the scenario with BPSK modulation, the application of the adaptation method reduces the bit error probability. This effect is most noticeable at high encoding rates

($\approx 9/10$), when the polar code corrects fewer errors, and their localization at the decoder input is more important.

Figure 10 shows the dependencies of BER performance when estimating $\hat{\mathbf{H}}$ with an error. Mean squared error (MSE, σ^2) ranges from 0 to 10^{-3} .

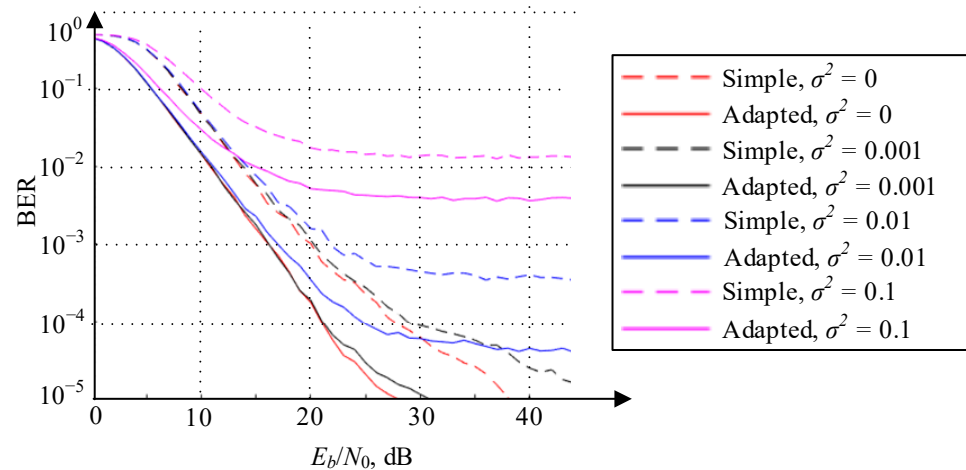


Figure 10. BER performance with different channel estimation error, $R = 1/2$.

As can be seen from Figure 10, the adaptation reduces the impact of the estimation error and significantly reduces BER. Thus, with $\sigma^2 = 10^{-1}$, the proposed method reduces BER by more than five times at high values of E_b/N_0 (more than 25 dB); with $\sigma^2 = 10^{-2}$ and $\sigma^2 = 10^{-3}$, BER is decreased by \approx eight times. In general, it can be noted that, despite the estimation error and, as a consequence, the incorrect sorting of physical subchannels in accordance with (14)–(18), the method does not lose efficiency and reduces BER.

A similar simulation was performed for NOMA (Figures 2 and 7) systems in accordance with the scheme shown in Figure 7. We considered the scenario of resource allocation between two UEs (UE1 and UE2). Upon that, UE1 and UE2 were located at the distances of 100 m and 200 m, respectively. The power between UE1 and UE2 was divided according to (8) in the ratio of $p_1 = 0.2$ and $p_2 = 0.8$. The other parameters corresponded to the OMA system. Figures 11–13 show the BER performance dependencies. For Figure 11: $K = 51$, $N = 512$ ($R \approx 1/10$); Figure 12: $K = 256$, $N = 512$ ($R \approx 1/2$); Figure 13: $K = 461$, $N = 512$ ($R \approx 9/10$).

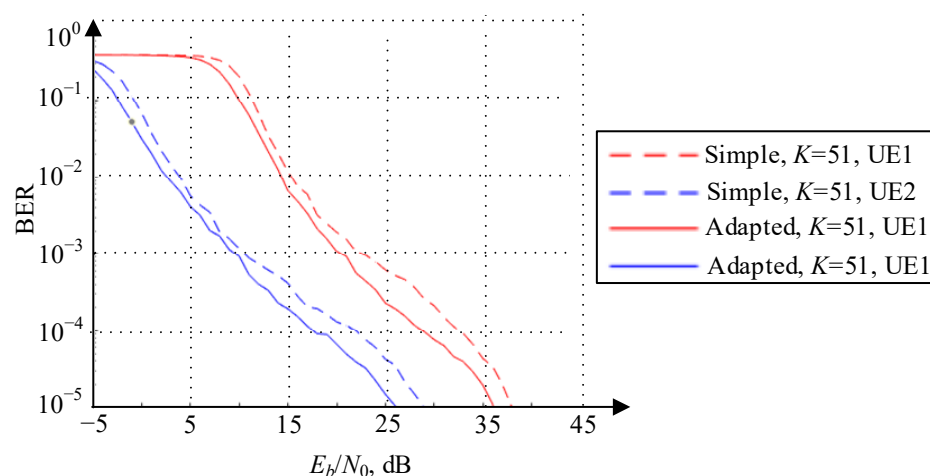


Figure 11. BER performance of NOMA system $K = 51$, $N = 512$.

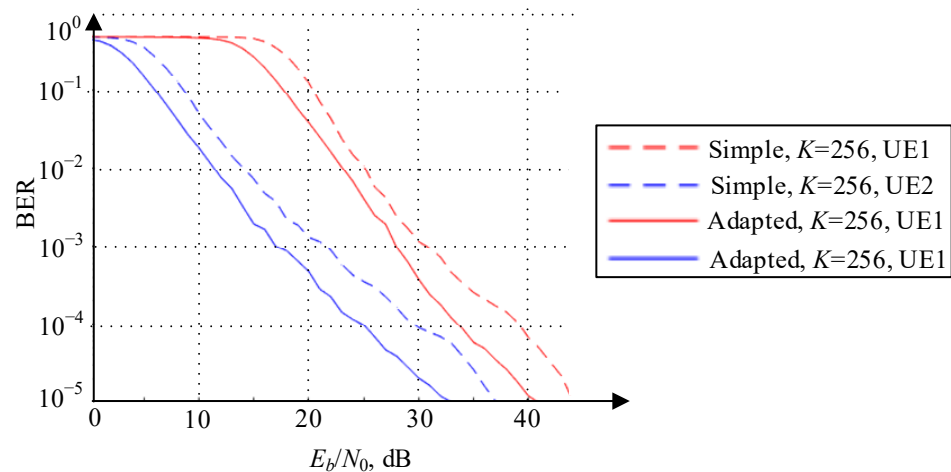


Figure 12. BER performance of NOMA system $K = 256$, $N = 512$.

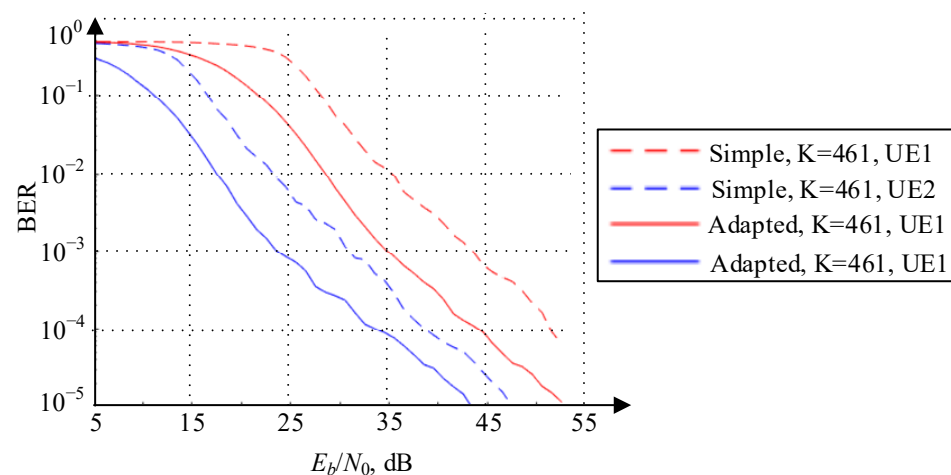


Figure 13. BER performance of NOMA system $K = 461$, $N = 512$.

As can be seen from Figures 11–13, the proposed method also works for NOMA scenarios. At the same time, both subscribers reduce the BER value as a result of the adaptation, regardless of the encoding rate. The gain value is from ≈ 3 to ≈ 5 dB

5. Conclusions

This article addresses the transmission of the signals of the OMA/NOMA systems with polar codes in multipath propagation channels. It proposes the method of adapting polar codes to the transmission conditions in the Rayleigh channels. The method is based on the distribution of logical channels over the OFDM physical subcarriers in relation to the fading depth of channel matrix \mathbf{H} .

The simulation results demonstrate the method efficiency and reduction in the bit error probability for various parameters of the encoding rate. We have considered the OMA systems with one transmitter and one receiver. In this scenario, the gain from the adaptation is from ≈ 3 to ≈ 5 dB. Receiver estimation error $\hat{\mathbf{H}}$ does not lead to a decrease in the method efficiency. On the contrary, the adaptation allows the reduction of the number of unrecoverable errors, depending on the error extent, from 5 ($\sigma^2 = 10^{-1}$) to 8 ($\sigma^2 = 10^{-2}$, $\sigma^2 = 10^{-3}$) times.

The application of the adaptation method for the NOMA scenario also demonstrates its efficiency. In all the scenarios considered (different encoding rates and two UEs), the adaptation provides the gain of up to 5 dB.

We shall expressly indicate that the proposed method involves interleaving bits and thus has a low computational complexity, which makes it easy to apply it in practice. This section is not mandatory but can be added to the manuscript if the discussion is unusually long or complex.

Author Contributions: Conceptualization, D.P.; methodology, D.P. and Y.K.; software, D.P., G.S. and A.S.; validation, Y.K. and E.R.; formal analysis, E.R.; investigation, D.P.; resources, D.P. and Y.K.; data curation, D.P.; writing—original draft preparation, D.P.; writing—review and editing, D.P. and E.R.; visualization, D.P.; supervision, S.N.; project administration, D.P.; funding acquisition, S.N. All authors have read and agreed to the published version of the manuscript.

Funding: The work has been completed with the financial support of the Ministry of Digital Development, Communications and Mass Media of the Russian Federation and Russian Venture Company (RVC JSC), as well as the Skolkovo Institute of Science and Technology, Identifier Subsidy's granting agreements 0000000007119P190002, No. 005/20 dated 26 March 2020.

Data Availability Statement: Not applicable.

Acknowledgments: The authors would like to thank the reviewers for their thoughtful remarks and recommendations, which considerably enhanced the paper's presentation.

Conflicts of Interest: The authors declare no conflict of interest.

References

1. Arıkan, E. Channel polarization: A method for constructing capacity achieving codes for symmetric binary-input memoryless channels. *IEEE Trans. Inf. Theory* **2009**, *55*, 3051–3073. [[CrossRef](#)]
2. 3GPP 38.212 V15.3.0; 3rd Generation Partnership Project (3GPP). Multiplexing and Channel Coding. 2018. Available online: https://www.etsi.org/deliver/etsi_ts/138200_138299/138212/15.03.00_60/ts_138212v150300p.pdf (accessed on 13 July 2022).
3. You, X.; Wang, C.; Huang, J.; Gao, X.; Zhang, Z.; Wang, M.; Huang, Y.; Zhang, C.; Jiang, Y.; Wang, J.; et al. Towards 6G wireless communication networks: Vision, enabling technologies, and new paradigm shifts. *Sci. China Inf. Sci.* **2021**, *64*, 1–74. [[CrossRef](#)]
4. Tong, J.; Wang, X.; Zhang, Q.; Zhang, H.; Li, R.; Wang, J.; Tong, W. Fast polar codes for terabits-per-second throughput communications. *arXiv Preprint* **2021**, arXiv:2107.08600.
5. Ping, Z.; Kai, N.; Hui, T.; Gaofeng, N.; Xiaoqi, Q.; Qi, Q.; Jiao, Z. Technology prospect of 6G mobile communications. *J. Commun.* **2019**, *40*, 141–148.
6. Ferris, A.J.; Hirche, C.; Poulin, D. Convolutional polar codes. *arXiv Preprint* **2017**, arXiv:1704.00715.
7. Trifonov, P. Efficient design and decoding of polar codes. *IEEE Trans. Commun.* **2012**, *60*, 3221–3227. [[CrossRef](#)]
8. Valerio, B.; Condo, C.; Land, I. Design of polar codes in 5G new radio. *IEEE Commun. Surv. Tutor.* **2020**, *23*, 29–40.
9. ETSI TS 138 141-1 V15.0.0 (2019-04) 5G NR; Base Station (BS) Conformance Testing Part 1: Conducted Conformance Testing (3GPP TS 38.141-1 version 15.0.0 Release 15)—3GPP. 2019; 200p. Available online: https://www.etsi.org/deliver/etsi_ts/138100_138199/13814101/15.00.00_60/ts_13814101v150000p.pdf (accessed on 13 July 2022).
10. Fayyaz, U.U.; Barry, J.R. Polar codes for partial response channels. In Proceedings of the 2013 IEEE International Conference on Communications (ICC), Budapest, Hungary, 9–13 June 2013.
11. Goela, N.; Abbe, E.; Gastpar, M. Polar codes for broadcast channels. *IEEE Trans. Inf. Theory* **2014**, *61*, 758–782. [[CrossRef](#)]
12. Zhou, D.; Niu, K.; Dong, C. Construction of polar codes in Rayleigh fading channel. *IEEE Commun. Lett.* **2019**, *23*, 402–405. [[CrossRef](#)]
13. Saito, Y.; Kishiyama, Y.; Benjebbour, A.; Nakamura, T.; Li, A.; Higuchi, K. Non-orthogonal multiple access (NOMA) for cellular future radio access. In Proceedings of the 2013 IEEE 77th Vehicular Technology Conference (VTC Spring), Dresden, Germany, 2–5 June 2013; pp. 1–5.
14. Nikopour, H.; Baligh, H. Sparse code multiple access. In Proceedings of the 2013 IEEE 24th Annual International Symposium on Personal, Indoor, and Mobile Radio Communications (PIMRC), London, UK, 8–11 September 2013.
15. Mao, Y.; Clerckx, B.; Li, V.O.K. Rate-splitting multiple access for downlink communication systems: Bridging, generalizing, and outperforming SDMA and NOMA. *EURASIP J. Wirel. Commun. Netw.* **2018**, *2018*, 1–54. [[CrossRef](#)]
16. Makki, B.; Chitti, K.; Behravan, A.; Alouini, M. A survey of NOMA: Current status and open research challenges. *IEEE Open J. Commun. Soc.* **2020**, *1*, 179–189. [[CrossRef](#)]
17. Liu, Y.; Zhang, S.; Mu, X.; Ding, Z.; Schober, R.; Al-Dhahir, N.; Hossain, E.; Shen, X. Evolution of NOMA toward next generation multiple access (NGMA) for 6G. *IEEE J. Sel. Areas Commun.* **2022**, *40*, 1037–1071. [[CrossRef](#)]
18. Diamanti, M.; Fragkos, G.; Tsiropoulou, E.E.; Papavassiliou, S. Unified user association and contract-theoretic resource orchestration in NOMA heterogeneous wireless networks. *IEEE Open J. Commun. Soc.* **2020**, *1*, 1485–1502. [[CrossRef](#)]

19. Diamanti, M.; Tsiropoulou, E.E.; Papavassiliou, S. The Joint Power of NOMA and Reconfigurable Intelligent Surfaces in SWIPT Networks. In Proceedings of the 2021 IEEE 22nd International Workshop on Signal Processing Advances in Wireless Communications (SPAWC), Lucca, Italy, 27–30 September 2021; pp. 621–625.
20. Chen, K.; Niu, K.; Lin, J. Improved successive cancellation decoding of polar codes. *IEEE Trans. Commun.* **2013**, *61*, 3100–3107. [[CrossRef](#)]
21. Tal, I.; Vardy, A. List decoding of polar codes. *IEEE Trans. Inf. Theory* **2015**, *61*, 2213–2226. [[CrossRef](#)]
22. Kryukov, Y.V.; Pokamestov, D.A.; Rogozhnikov, E.V. PD-NOMA power coefficients calculation while using QAM signals. In *International Conference on Distributed Computer and Communication Networks*; Springer: Cham, The Netherlands, 2019.
23. Kryukov, Y.V.; Pokamestov, D.A.; Abenov, R.R.; Mukhamadiev, S.M.; Kanatbekuli, I. Spectral efficiency analysis of two-user Downlink PD-NOMA with LTE modulation and coding schemes. *J. Phys. Conf. Series* **2021**, *2134*, 1. [[CrossRef](#)]
24. Rugini, L.; Banelli, P.; Leus, G. Simple equalization of time-varying channels for OFDM. *IEEE Commun. Lett.* **2005**, *9*, 619–621. [[CrossRef](#)]